# Analytical and Numerical Investigations of Refined Macroscopic Traffic Flow Models

M. Herty* R. Illner†

June 18, 2009

**Abstract**

We continue research on generalized macroscopic models of conservation type as started in [15]. In this paper we keep the characteristic (for traffic) nonlocality removed in [15] by Taylor expansion and discuss the merits and problems of such an expansion. We observe that the models satisfy maximum principles and conclude that "triggers" are needed in order to cause traffic jams (braking waves) in traffic guided by such models. Several such triggers are introduced and discussed. The models are refined further in order to properly address non-monotonic (in speed) traffic regimes, and the inclusion of an individual reaction time is discussed in the context of a braking wave. A number of numerical experiments are conducted to exhibit our findings.

## 1 Introduction

In [15] we derived macroscopic models of Aw-Rascle [1] and Zhang [33] (and related) type from Vlasov-type kinetic models and explored their properties. In this sequel we revisit and refine these models, analyse them further and present a number of numerical simulations. As in [15] we start with a quite general kinetic equation of Vlasov-type and arrive at corresponding moderate to high density macroscopic models by inserting the ansatz $f(x,v,t) = \rho(x,t)\delta(v-u(x,t))$. The models inherit time delays (due to reaction times) and nonlocalities (due to driver behaviour) from the microscopic (or kinetic) assumptions.

In [15] we ignored individual reaction times but included nonlocal behaviour (which, we believe, is *the most essential* feature in traffic interactions). The corresponding macroscopic models look promising but are hardly accessible to standard analytical techniques. Therefore, we eliminated the nonlocalities by Taylor expansions, truncating after second order terms (a questionable step, as the displacement distances arising in the nonlocal terms can be significant). The resulting system of equations (continuity equation, plus two types of momentum equations depending on whether one is in a braking or acceleration scenario) were found to possess traveling wave solutions that seem to reflect well how braking or acceleration waves propagate in dense traffic.

In the present paper we revisit these issues. Specifically, we address the following in Section 2.

- We include the individual reaction time in our analysis. This leads to a minor modification of the original model.

*RWTH Aachen University, D-52056 Aachen, Germany. herty@mathc.rwth-aachen.de, Phone. +492418096954, Fax. +492418093920

†Department of Mathematics and Statistics, University of Victoria, PO Box 3045 STN CSC, Victoria, B.C., Canada V8W 3P4. rillner@math.uvic.ca, Phone. +12507217456, Fax. +12507218962

- A simple Taylor expansion argument shows that the dependencies of specific braking and acceleration forces on the macroscopic density and relative speed used in [15] are to be expected even for a class of more general models.

- We next focus on a deceleration (braking) secenario and use a traveling wave ansatz to derive a differential equation with an appropriate nonlocality (the "jam" equation). The equation allows all constants as trivial solutions, but the existence of nontrivial solutions ("braking" waves) is an open (and challenging) question. We suspect that such waves exist and are actually the asymptotic states reached in sufficientlty dense traffic after a traffic jam is caused by a "trigger." Our numerical experiments (see below) provide evidence for this.

  Eliminating the nonlocality by an expansion as in [15] but retaining the reaction time $\tau$, one finds ODEs similar to those in [15], but the individual reaction time remains as an additional parameter. For this reduced model it is easily seen that traveling waves exist, and their qualitative features show a weak dependence on $\tau$. We derive constraints on the wave speed $V$ in terms of the other parameters.

- We present numerical results on the full model including the non–local term, generalizing preliminary work from [15] where we only presented numerical results on traveling wave solutions for a model where the nonlocality was removed by expansion. In particular, here we correct a conceptual mistake contained in [15]: The results presented in Figures 3 and 4 in that paper are flawed in the sense that the depicted waves were obtained by solving the ODEs for traveling wave solutions; the problem is that the given data are in general not consistent with traveling wave solutions, and in order to obtain the proper solution, the full system must be solved. We regret this error, and its correction is one of the jobs done here.

Section 3 contains some analysis with consequences for the modeling:

- All our models satisfy maximum principles in the sense that if an initial speed profile takes values in $[u_{min}, u_{max}]$, then so will the solution. This is easy to see and raises the question how traffic jams start. The answer is that the start of a jam is not provided by the model: one needs a "trigger", an event which causes sudden braking of one or many drivers in response. Triggers can be the spatial or temporal introduction of a speed limit; or a braking reaction of drivers to a sudden density concentration (measured as a diminished distance to the lead car—in practice, this could be caused by a single driver who brakes in order to increase his/her distance to the lead car); or a density jump due to a lane ending or traffic accident. Everyone who has ever driven on a highway has probably experienced one of these triggers.

- These issues are explored in a series of numerical experiments in Section 4. In particular, we estimate wave speeds of moving jams ("braking waves") in response to an initially present deceleration profile. The response depends on the initial size of the (constant) car density: For low densities, the deceleration profile moves forward in traffic direction and steepens. For high densities the profile moves backwards and appears to be well approximated by a traveling wave, with growing accuracy for higher densities. We perform numerical tests to this end and also use the scenario to compare these numerical solutions of the problem with traveling wave solution of the reduced ("localized" by Taylor expansion) jam equation. This comparison shows that the Taylor expansion introduces a significant error. Furthermore, we discuss triggers: In Section 4.2 we consider sudden temporal changes in the local speed variable (modeling random braking scenarios), changes in the

initial density as model for lane reduction or accidents, and speed limits imposed on parts of the road. In all these cases we observe density-dependent traffic jams in the form of backward-moving traveling waves.

Our results offer the prospect of analytical and numerical explorations of optimal traffic control in response to the characteristic parameters (reaction time, safety distance, characteristic braking and acceleration times). For example, what speed limit will offer maximal flow and absence of stop-and-go waves while providing safety? Numerical experiments to this end are projected for the future.

We conclude this introduction by a (very) brief review of other approaches to traffic modeling. Indeed, our models belong to only one class of possible models and ignore aspects of traffic such as variations in vehicle size and mass, driver behaviour, random fluctuations, etc. While it is possible to include such effects, our first priority here is simplicity in order to identify basic structures and explain arising phenomena.

Our model is a macroscopic model derived from a Fokker–Planck ansatz, see [20, 15, 16, 19]. Macroscopic models have been studied intensively in recent years and an incomplete list of references include [1, 3, 4, 8, 9, 10, 11, 17, 23, 25, 27, 33, 12, 18]. Second order macroscopic models use equations similar to fluid dynamics models to describe the evolution of traffic density and velocity profiles. In contrast, microscopic models keep track of individual drivers and their interactions in order to explain traffic phenomena. Some references on microscopic models are [6, 7, 13, 14, 22, 32, 28, 29]. Microscopic models can take the form of systems of ordinary differential-delay equations, or of discretized versions such as cellular automata. These models have been extended to include stoachstic effects, see e.g., [26], [30, 31]. Finally, there is a class of kinetic models of Enskog–type which relates to microscopic and macroscopic models, see e.g. [21].

# 2 Modeling

## 2.1 From Kinetic Equations of Vlasov Type to Macroscopic Models

Throughout this paper $x, v, t$ will denote position (on the road), speed $\in [0, \infty)$, and time.
$f = f(x, v, t)$, $\rho = \rho(x, t), u = u(x, t)$ denote the kinetic density, the macroscopic density and the macroscopic (average) speed of cars on a highway (freeway) lane. As lane changing in high density is difficult, it is rare (sometimes, of course, you have to change lanes) and hence disregarded. Our analysis is therefore confined to one lane or to a lane-homogenized scenario. By definition, we have the relationships

$$\rho(x,t) = \int f(x,v,t)\ dv, \quad (\rho u)(x,t) = \int v f(x,v,t)\ dv.$$

As the reaction of drivers is always driven by what they see ahead of themselves, we introduce the shorthand

$$\mathbf{u}^X(x,v,t) = u(x + H + Tv, t - \tau),$$

for the nonlocal average velocity at the point $x + H + Tv$ and time $t - \tau$. Here, $H$ is considered a minimal safety distance, $\tau$ is the "individual" reaction time, and $T$ is a characteristic reaction time which multiplies the driver's speed. We choose one constant value of $T$ for both braking and acceleration scenarios. In practice, one could (and should) use two different values $T_B < T_A$ for braking and acceleration, and a trivial modification of our modeling will accommodate for this. Note how the (independent) speed variable enters into the macroscopic variables through this definition.

Our Vlasov model for high density traffic with a braking/acceleration force $B$ (and without diffusion) is

$$\partial_t f(x,v,t) + v\partial_x f(x,v,t) + \partial_v\Big(B\left(\rho(x,t), v - \mathbf{u}^X(x,v,t)\right) f(x,v,t)\Big) = 0 \tag{1}$$

where we are making the implicit assumption that $B$ depends only on the density (at $(x,t)$) and at the relative speed (with respect to $\mathbf{u}^X$) of the reference vehicle at $(x,v)$. The detailed behaviour of the model depends, of course, on the assumptions made for $B$. The characteristics of this model are the microsopic rules for cars given by

$$x'(t) = v,\ v' = B(\rho, v - \mathbf{u}^X).$$

As in [15] we will consider the choice

$$B(\rho, v - \mathbf{u}^X) = \begin{cases} -g_1(\rho)(v - \mathbf{u}^X) & \text{if} \quad v - \mathbf{u}^X > 0 \\ -g_2(\rho)(v - \mathbf{u}^X) & \text{if} \quad v - \mathbf{u}^X < 0 \end{cases} \tag{2}$$

where $g_2(\rho)$ should be a decreasing function of $\rho$. Although more complicated choices are possible and will be discussed later on, we proceed with the setting

$$g_1(\rho) = c_1\rho, \quad g_2(\rho) = c_2(\rho_{max} - \rho).$$

This $B$ was used in [16] to study long–time behavior of solutions. For this particular choice the braking force $B$ is assumed proportional to the density as well as the speed difference to the lead car. The acceleration is proportional to the speed difference and antiproportional to the car density. There is no acceleration as the maximum density is reached, a reasonable assumption.

The above ansatz for the braking and acceleration forces follows naturally from a second-order Taylor expansion, as we show below and was already discussed in [15].

To proceed to macroscopic models, let $\phi \in C_0^\infty((-\infty,\infty)\times(0,\infty)\times(0,\infty))$ be a test function, $\phi = \phi(x,v,t)$. The function $f(x,v,t)$ is called a weak solution of (1) if for all such $\phi$

$$T_f(\phi) := \int\int\int \phi_t f + \phi_x v f + \phi_v(B(\rho, v - \mathbf{u}^X)f)dx\ dv\ dt = 0. \tag{3}$$

**Proposition 1.** *The distribution valued function $\rho(x,t)\delta(v - u(x,t))$ is a weak solution of (1) in the sense of (3) if and only if almost everywhere*

$$\rho_t + (\rho u)_x = 0 \tag{4a}$$

$$\rho\left(u_t + uu_x - B(\rho, u - u^X)\right) = 0 \tag{4b}$$

*where the function $u^X(x,t)$ is here defined by $u^X(x,t) := u(x + H + Tu(x,t), t - \tau)$.*

The proof of this Proposition is given in [15]. This is an elementary way of "deriving" a macroscopic from a kinetic model.

## 2.2 On Braking and Acceleration forces

The $B$ used in our Vlasov equation can be completely general. However, reasonable assumptions on the dependencies of $B$ lead naturally to forces such as used in (2). First, consider a braking scenario. If we abbreviate $w := u - u^X$, this means $w > 0$. Then $B = B(\rho, w)$, and it is natural to assume that

$$B(\rho, 0) = 0 \quad \forall \quad \rho \in [0, \rho_{max}] \tag{5}$$
$$B(0, w) = 0 \quad \forall \quad w \leq 0 \tag{6}$$

(if a reference driver moves with the same speed as the lead car, there is no need for braking–there may be acceleration, but let us ignore that for now); if the density is zero, i.e., if there are no other cars in front of you, there is again no need for braking (there may be acceleration). These assumptions readily entail that

$$B(0,0) = \partial_\rho B(0,0) = \partial_{\rho\rho} B(0,0) = 0,$$

and

$$\partial_w B(0,0) = \partial_{ww} B(0,0) = 0.$$

Assuming that $B$ can be expanded in a Taylor series, we find to second order

$$B(\rho, w) = B_{\rho w}(0,0)\rho w.$$

Setting $c_1 = -B_{\rho w}(0,0)$ this is exactly the ansatz used in (2).

A similar discussion applies to the acceleration scenario; abbreviating (for now) the acceleration force by $A = A(\rho, w)$ where $w < 0$ we observe $A(\rho_{max}, w) = 0$ and $A(\rho, 0) = 0$. The formal second order expansion gives

$$A(\rho, w) = c_2(\rho_{max} - \rho)w$$

which was used in [15].

It must be stated at this point that these assumptions are simplistic, especially for the acceleration case. There are driver behaviours which are ignored at this point and which we will discuss later in this work, such as spontaneous acceleration in low density traffic, spontaneous braking in high densities, and general "noisy" driving. The assumptions made above assume simply that the only relevant variables are the density and the relative speed to the lead car as observed by the reference driver. Furthermore, it is not realistic to set $A(\rho_{max}, w) = 0$ for all $w < 0$ and $A(\rho, 0) = 0$ for small $\rho$. The first assumption ignores the fact that acceleration can (and will) occur even in high densities if the lead car begins to move on; the second ignores that at low density one can (and will) accelerate even if the lead car (which is far ahead) moves at one's own speed or even more slowly. Modifications to these rules are easily envisioned, introduced and implemented, and they give rise to acceleration "triggers" as seen (later) in our numerical examples.

## 2.3 "Jam" equations and braking waves.

For this subsection we focus on a braking regime where $u_x < 0$ (a remarkable feature of traffic modeling is that model switches depending on properties of the solutions themselves are realistic and required). The model equations (4) read

$$\rho_t + (\rho u)_x = 0 \tag{7}$$
$$u_t + u_x u + c_1 \rho (u - u^X) = 0 \tag{8}$$

with $u^X(x,t) = u(x + H + Tu(x,t), t - \tau)$. A traveling wave ansatz (as in [15]) $\rho(x,t) = \rho(x + Vt)$, $u(x,t) = u(x + Vt)$ and the shorthand $s := x + Vt$ leads to the ODEs

$$\frac{d}{ds}(\rho(u + V)) = 0 \tag{9}$$

and

$$(V + u)u'(s) + c_1\rho(s)\,(u(s) - u(s + (H - \tau V) + Tu(s))) = 0. \tag{10}$$

Each traveling wave solution of our (braking) model satisfies (9) and (10), and conversely, each solution of these equations with $u'(s) < 0$ for all $s$ is a traveling wave solution of the model.

Equation (9) immediately integrates to $\rho(s)(u(s) + V) = c_0V$ (the factor $V$ on the right is kept for convenience), and after insertion into (10) we obtain

$$(u + V)^2u'(s) = -c_1c_0V\,[u(s) - u(s + (H - \tau V) + Tu(s))]\,. \tag{11}$$

Assuming that in the traveling wave regime $u = 0$ if $\rho = \rho_{max}$, we find $c_0 = \rho_{max}$. This is the value of $c_0$ used in [15], and it appears reasonable. However, other values of $c_0$ support other traveling wave solutions and should not be discarded from the outset.

We refer to this type of equation as a "**jam**" equation. Based on numerical experiments presented later in this paper we believe that it describes how braking waves triggered in dense traffic will propagate through traffic. Observations suggest that in dense traffic $V$ will be positive and of the order of magnitude of 10–20 $km/h$, so that braking waves will propagate backwards through traffic with such speeds.

A comment. If we set $z(s) := u(s) + V$ and abbreviate $c_V := H - (T + \tau)V$ then equation simplifies to

$$\frac{d}{ds}(\frac{1}{3}z^3) = c_1c_0V\,[z(s + c_V + Tz(s)) - z(s))] \tag{12}$$

This looks simple and intriguing, but we know of no tools to solve it analytically (except, of course, for nontrivial constant solutions). Recall that a necessary condition for the usability of these equations is $z'(s) \leq 0$. The solvability and solution properties of (12) are open and an interesting prospect, especially in terms of their dependence on the parameters.

It is completely natural to reduce the analytical complexity of (11) by removing the nonlocality via a Taylor expansion. However, the dimension of the nonlocalities is significant. If we measure distance in metres, time in seconds and if we take $H = 8m, \quad T = 2sec$, then at a speed $u = 15m/sec$ we find $H + Tu = 38m$. That is, in a braking scenario there should be a distance of 38 metres from the front of your car to the front of the lead car if traffic moves at 54 $km/h$. These 38 metres are not a small quantity and do not a priori justify Taylor's expansion in terms of $H + T\,u$. In [15] we used the expansion anyway in order to obtain a solvable problem. We repeat this and include the individual reaction time for completeness.

After expanding $u$ in (11) to second order ($u(s + (H - \tau V) + Tu(s)) = u(s) + u'(s)(H - \tau V + Tu(s)) + (1/2)(H - \tau V + Tu(s))^2 + \ldots)$), substitution and truncation of the higher order terms, the jam equation becomes

$$\frac{d^2u}{ds^2} = 2\frac{(u + V)^2 - c_1c_0V(H - \tau V + Tu)}{c_1c_0V(H - \tau V + Tu)^2}\frac{du}{ds}. \tag{13}$$

For $\tau = 0$ this is identical to the braking equation we studied in [15]. In fact, we have obtained the same equation with a small change of parameter ($H$ has changed to $H - \tau V$). As in [15] one can check that braking waves ending at a small (positive) residual speed $u_0$ will exist if the wave speed $V$ satifies

$$0 \leq V < \frac{c_1 c_0 H}{1 + c_1 c_0 \tau} < H/\tau.$$

These braking waves are best depicted in phase space $\{(u, u')\}$. A numerical integration of (13) is depicted in Figure 2.3 for a set of parameters as in table 1 and initial data of $u(0) = 80\%\ u_{\max} = 24\frac{m}{s}$ and $u'(0) = -10\%\ 8\frac{m}{s^2}$.

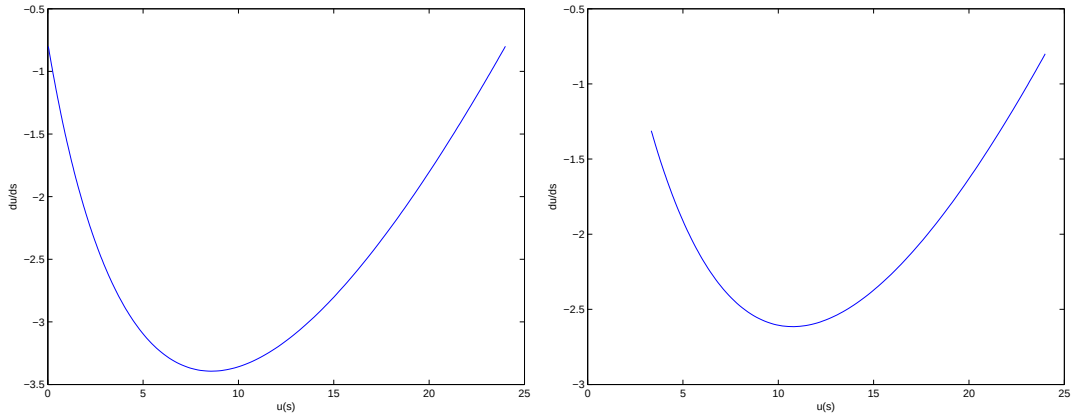


Figure 1: Numerical integration of (13) depicted in the $u - u'-$phase space for different reaction times $\tau = \frac{1}{4}\ sec$ (left) and $\tau = 0$ (right).

A similar derivation holds for the acceleration case, leading to a "rarefaction" equation. We omit the details.

# 3 Maximum Principles, Model Refinements and Triggers

## 3.1 Maximum Principles

Let us assume that traffic flows according to the equations

$$\rho_t + (\rho u)_x = 0 \tag{14}$$

$$u_t + u u_x + c_1 \rho (u - u^X) = 0 \text{ while } u - u^X \geq 0 \tag{15}$$

$$u_t + u u_x + c_2 (\rho_{max} - \rho)(u - u^X) = 0 \text{ while } u - u^X < 0 \tag{16}$$

and assume that we have a (smooth) solution $\rho(x,t), u(x,t)$ such that at $x_0$

$$u(x_0, t) = \sup_{x, s \leq t} u(x, s).$$

A driver at $x_0$ at time $t$ will then be in a braking situation, and one easily sees that $u_t(x_0, t) \leq 0$. A driver at a location $x_0 - \delta$ at time $t$ may be in an acceleration situation, but the acceleration law will not allow to accelerate past the maximal value of $u$. Similar considerations apply to minimal speed values, and we observe that our models (in fact, every model whose acceleration and braking forces are proportional to the relative speeds with respect to the lead car) will obey a maximum principle:

**Proposition 2.** *Suppose that for all $x$ and all $s \in [0,\tau]$ we have*

$$0 \le a \le u(x,s) \le b.$$

*Then for any smooth solution of (16)*

$$0 \le a \le u(x,t) \le b$$

*for all $x$ and all $t \ge 0$.*

This principle is consistent with the trivial fact that every constant state $(\rho, u)$ is a solution of our model equations; and there will be no deceleration below the lowest speed driven anywhere on the road at time zero, and no acceleration beyond the fastest such speed.

Reality shows us every day that this is not realistic. Traffic jams occur and disappear in steady dense traffic for (sometimes) no apparent reason, such jams usually lead to standing traffic, etc. Our models need refinement in order to account for such effects.

### 3.2 Refinements and Triggers.

It is not hard to understand which features our modeling process has ignored so far. They are features of two different flavours.

- More careful modeling of the braking/ acceleration forces in regimes where the speed profile is not monotone. This arises, for example, in a neighborhood of local speed maxima or minima, or in regimes where the speed profile is rather oscillatory with short "wavelengths" (whether such regimes arise in practice is a separate question). For example, assume that there is a $\sigma$ such that

  $$0 < \sigma < H + Tu(x,t) \qquad \text{and} \qquad u(x,t) > u(x+\sigma,t),$$

  but $u(x,t) < u(x + H + Tu(x,t))$. According to our models, the reference driver at $x,t$ will act as if he/she is in an acceleration scenario although there are slower vehicles immediately in front of him/her. The problem is obvious: The nonlocality scale in this case exceeds the monotonicity domain. Remedies for this are immediately clear once the problem is realized:

  We redefine

  $$\rho^X = \sup_{\sigma \in (0, H+Tu(x,t))} \rho(x+\sigma, t-\tau), \tag{17}$$

  $$u^X = \inf_{\sigma \in (0, H+Tu(x,t))} u(x+\sigma, t-\tau), \tag{18}$$

  $$\bar{u}^X = u(x + H + Tu(x,t), t-\tau) \tag{19}$$

  (note that $\bar{u}^X = u(x + H + Tu(x,t), t-\tau)$ is what was previously called $u^X$) and

  $$B(\rho, u, u^X) = \begin{cases} -c_1 \rho^X (u - u^X) & \text{if } u - u^X > 0. \\ -c_2(\rho_{\max} - \rho^X)(u - \bar{u}^X) & \text{if } u - u^X \le 0. \end{cases} \tag{20}$$

  The new braking law uses the maximal observed density and the minimal observed speed in the relevant window; only if $u - u^X \le 0$ is the braking case rejected, and then we accelerate according to the old rule.

  There is certainly more flexibility to modify these rules. In fact, we discovered the necessity of modification by numerical experiments, in which the original rules led to unrealistic density and speed oscillations due to the scale problem mentioned above.

- These revisions are still consistent with the validity of a maximum principle as discussed earlier (in fact, in monotone regimes the modifications amount to no model changes at all). This leaves the task of introducing triggers; an open-ended task, because in reality there are undoubtedly many different triggers. For the purpose of this paper we will only consider two triggers, one requiring a structural model change, the other requiring temporally and spatially localized rule changes, for example by a speed limit.

  First, let us assume that drivers will be uncomfortable driving at high speed in dense traffic (this is certainly realistic). Suppose that a driver will feel the need to reduce speed if the observed density ($\rho^X$) exceeds a certain multiple of the "comfort density" $\rho_c := 1/(H+Tu)$ which is relevant for a braking event. In other words, we assume that there is a constant $c_3$ such that a driver will spontaneously brake if $\rho^X(H+Tu) \geq c_3$, and the braking force will not be dependent on relative speeds, but be proportional to $\rho$ and to $u$. This leads to

$$B(\rho, \rho^X, u-u^X) = \begin{cases} -c_1\rho u & u-u^X > 0, \rho^X(H+Tu) \geq c_3 \\ -c_1\rho(u-u^X) & u-u^X > 0, \rho^X(H+Tu) \leq c_3 \\ -c_2(\rho_{\max}-\rho)(u-\bar{u}^X) & u-u^X < 0, \rho^X(H+Tu) \leq c_3 \\ 0 & u-u^X < 0, \rho^X(H+Tu) \geq c_3 \end{cases} \tag{21}$$

  Note that the second and third lines reproduce the previous model in case of moderate density. The final line states that no acceleration occurs in high densities, even though the relative speeds are consistent with acceleration.

  Other modifications are possible, e.g., we could make the braking force proportional to $\rho^X$ instead of $\rho$. It is also possible to think of other weights for the strength of the acting forces, e.g., replacing $-c_1\rho u$ by $-c_1\rho^\gamma u^\kappa$ for some exponents $\gamma, \kappa \geq 1$. However, since all these quantities might be difficult to observe from data we kept the model simple and only use a priori given parameters as, for example, the safety distance $H$ and the reaction time.

**Remark 1.** *The braking force $-c_1\rho(u-u^X)$ which applies in (21) has interesting effects in the numerical simulations. For example, consider a spontaneous braking scenario: free flow traffic at constant speed and density, and at $t=0$ a single car at some position $x_0$ brakes. At time $\tau$ the cars at positions $[\tilde{x}_0, x_0]$ with $\tilde{x}_0 := x_0-(H+Tu)$ observe the change in velocity and begin to brake. Since $u^X = \inf_\sigma u(x+\sigma, t-\tau)$ the braking force will be the* same *for all cars in $[\tilde{x}_0, x_0]$. This forces a discontinuity in $u$ at $\tilde{x}_0$ which in turn leads to a concentration in the density. Furthermore, we observe secondary effects: at time $2\tau$, cars in $[\tilde{x}_0-(H+Tu), \tilde{x}_0]$ start to brake and so on. These effects are visible in the numerical simulations depicted in Figure 9 and Figure 11.*

# 4 Numerical Experiments

We present numerical results for (4) in conservative form

$$\rho_t + (\rho u)_x = 0 \tag{22a}$$

$$(\rho u)_t + (\rho u^2)_x = \rho B(\rho, u-u^X) \tag{22b}$$

together with braking and acceleration terms as discussed in the previous section. More precisely, we present results using either

$$B(\rho, u, u^X) = \begin{cases} -c_1\rho(u-u^X) & u-u^X > 0. \\ -c_2(\rho_{\max}-\rho)(u-\bar{u}^X) & u-u^X < 0. \end{cases} \tag{23}$$

or

$$B(\rho, u-u^X) = \begin{cases} -c_1\rho u & u-u^X > 0, \rho^X(H+Tu) \geq c_3 \\ -c_1\rho(u-u^X) & u-u^X > 0, \rho^X(H+Tu) \leq c_3 \\ -c_2(\rho_{\max}-\rho)(u-\bar{u}^X) & u-u^X < 0, \rho^X(H+Tu) \leq c_3 \\ 0 & u-u^X < 0, \rho^X(H+Tu) \geq c_3 \end{cases} \tag{24}$$

The system of balance laws (22) is numerically solved by a first–order finite volume method on a uniform grid with $N_x$ grid points in space. We apply a first–order time–splitting approach to treat the source term. The transport part consists of the equations of pressureless gas dynamics. A Godunov scheme in the conservative variables $(\rho, \rho u)$ for these equations can be found in [24] and has been discussed therein. We use precisely this scheme for discretization of the transport. Time and spatial discretization are choosen such that the CFL condition is satisfied. Alternative discretizations can be found in [2] or the references therein. Higher–order spatial and temporal discretizations could also be used in order to solve the equations numerically. However, since the problem is one–dimensional in space the computational time even on very fine grids is within minutes. The source term $\rho B(\rho, u-\mathbf{u}^X)$ is evaluated at the center of each cell with piecewise constant reconstruction of $\rho$ and $u$. To compute $\mathbf{u}^X$ we interpolate $u$ using the nearest neighbor. Since the source term is non–stiff a first–order explicit Euler scheme for the integration of the source term with a temporal discretization given by the transport part is sufficient. If not stated otherwise we set up a "circular" road (using periodic boundary conditions) and use parameter values as given in table 1. Initial data is prescribed as discussed below. All computations have been performed on a 2.4 GHz Intel Core 2 Duo.

| | |
|---|---|
| Length of the road | 2000 |
| Savety distance $H$ | 10 |
| Time $T$ | 2 |
| Reaction time $\tau$ | 1 |
| Maximal density $\rho_{\max}$ | $2/H$ |
| $c_1$ | $1.6/\rho_{\max}$ |
| $c_2$ | $1/\rho_{\max}$ |
| $c_3$ | 1 |

Table 1: Parameters used in the traffic flow model. All distances are in meters and all times in seconds.

## 4.1 Experiments for Models (4), (23) and (4), (24)

### 4.1.1 Test of the Spatial Discretization- "Calibration"

For $B \equiv 0$ the traffic flow model is exactly the system of pressureless gas dynamics, and we reproduced numerical experiments done elsewhere to test our methods. In order to verify our numerical scheme we used benchmark calculations for Example 2 in [2]. In this test problem two compactly supported clouds collide and produce a $\delta-$wave in the density. We use $N_x = 1600$ points in space and initial data prescribed at $t = -1$ as in [2]

$$(\rho(x,-1), u(x,-1)) = \begin{cases} (2,1) & -2 < x < -1 \\ (1,-1) & 1 < x < 5 \\ (0,0) & \text{else} \end{cases} .$$

Since the solution contains a $\delta-$wave in the density we adjust the plotting area for the density (as in [24]) as follows: we only show densities below 3.5. As expected, the two clouds collide at time $t = 0$

and the left cloud gives rise to a concentration in density at at time $t \approx 1.21$. More details as well as the analytial solution to this problem can be found in Section 4 of [24]. We depict the solution at time $t = 0.5$ and $t = 1.5$ in Figure 2 and observe a good agreement of the expected wave speeds.

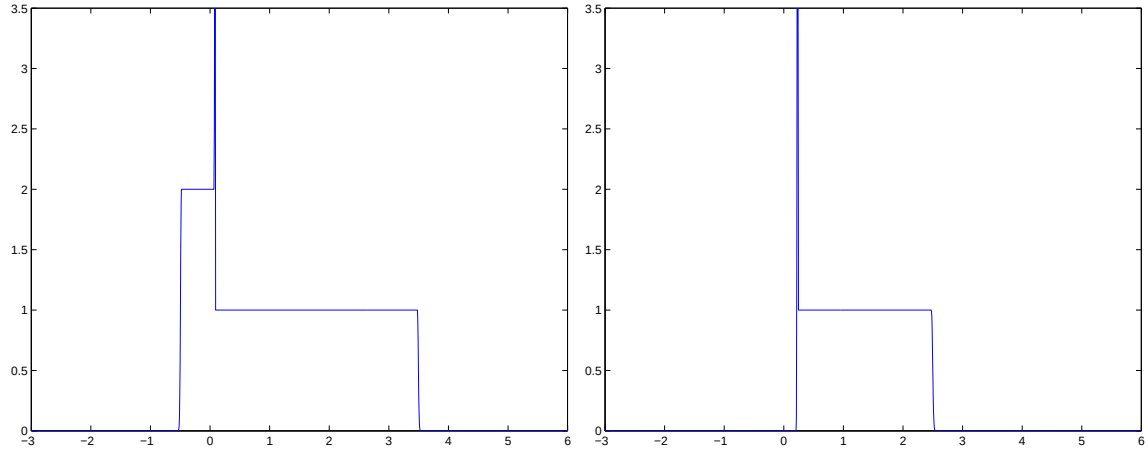

Figure 2: Pressureless gas dynamics with two colliding clouds at time $t = 0.5$ and $t = 1.5$. Density profiles are shown. The plot is restricted to the values where $\rho \leq 3.5$

### 4.1.2 On Wave Formation, Propagation and Speed

For the model with braking term (23) we ran simulations using different (constant) initial densities ranging from 6.6% to 33.3% of the maximal density. The initial velocity was chosen to decay smoothly (using a hyperbolic tangent profile) from $24m/s$ to $5m/s$ over a distance of 400 m. All simulations produced (in $u$) a wave similar in structure to the initial profile, but depending on the initial chosen density it moved with either negative or positive velocity, see figure 3. For higher densities the wave moves backwards, whereas in regions of low density the wave moves forward and becomes steeper. Numerical estimates of the wavespeeds are presented in table 2.

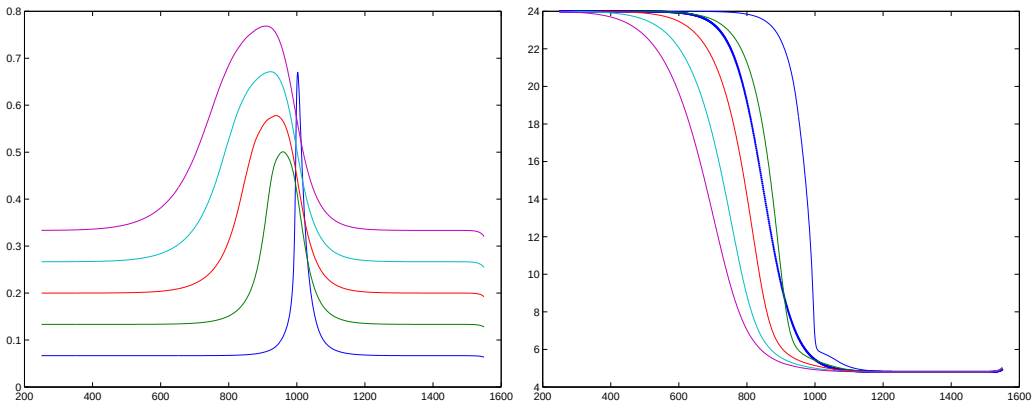

Figure 3: Traveling waves obtained by simulating (23) for an initial velocity profile as depicted in bold blue in the picture to the right. The density is initially constant. Same colours are corresponding solutions. The solutions are depicted at time $T = 20sec$.

| $\rho$ | $V$ |
|---|---|
| 6.6e-2 | -6.3 |
| 1.3e-1 | -1.0 |
| 2.0e-1 | 2.55 |
| 2.6e-1 | 5.65 |
| 3.3e-1 | 8.30 |

Table 2: Approximate wave speeds $V$ in $m/s$ of the braking waves in $u$ (simulated with the braking force (23)) from the corresponding solutions as depicted in figure 3.

We investigated whether the emerging profiles match traveling waves in the relevant domains. These domains depend on the initially chosen densities and the corresponding wave speed $V$. For the lowest initial density ($\rho_0 = 0.066$, measured as a fraction of the maximal density) no traveling wave profile can be discerned after $T = 20$ seconds; in fact, the steepening of the profile suggests approximation to a shock wave, although we were not able to prove this analytically. For the initial density $\rho_0 = 0.26$ and the corresponding estimated speed $V = 5.65$ we entered the data between road coordinates 600 and 900 into the left hand side of the continuity equation in traveling wave form (9) and computed $\frac{d(\rho(u+V))}{ds}$. The result is shown in Figure 4 and shows that the equation is satisfied up to errors of order $3.5 \times 10^{-3}$. This calculation required no choice of $c_0$.

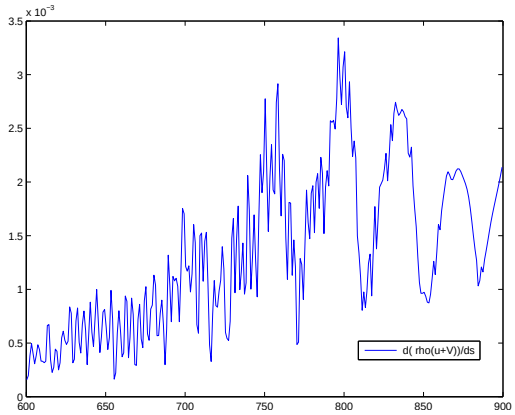


Figure 4: The function $s \to |d(\rho(u+V))/ds|$ with $\rho(x,T)$ and $u(x,T)$ as the solutions to (23) with initial density $\rho_0 = 0.26$ and $u_0$ as in Figure 3 at time $T = 20sec$.

We then estimated a suitable $c_0 = 1.35\rho_{max}$ by optimally matching the data curve for $\rho$ and the traveling wave approximation $\frac{c_0 V}{u+V}$ (where u is taken from the data set), see Figure 5.

We then entered the data for $\rho$ and $u$ into the traveling wave form of (10) and (11) with the previously chosen $c_0$. The results are shown in Figure 6 where $\frac{du}{ds}$ is obtained numerically using centered finite differences which explains the small oscillations.

The results of Figure 6 suggest that the approximation by a traveling wave in the domain [600,900] is excellent.

We then repeated this test for initial $\rho = .2$ and the corresponding $V = 2.55$ in the same domain. Here the test produces a significantly larger error, which suggests that either no traveling wave forms at all, or it takes a much longer time to get there. Our numerical tests to date are insufficient (because of the periodic boundary conditions) to decide this. We omit the pictures.

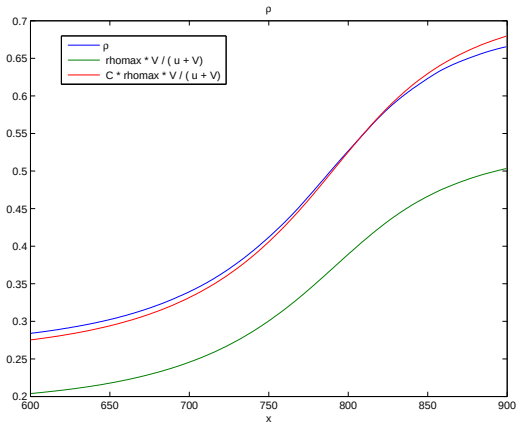


Figure 5: Density $\rho(x,T)$ as solution to (23) at time $T = 20sec$ in comparison with the functions $x \to \frac{\rho_{max} V}{u(x,T)+V}$ and $x \to \frac{C\rho_{max} V}{u(x,T)+V}$ for $C = 1.35$ and $u(x,T)$ being the solution to (23) at time $T = 20sec$. A restriction of the area $600 \leq x \leq 900$ is shown.

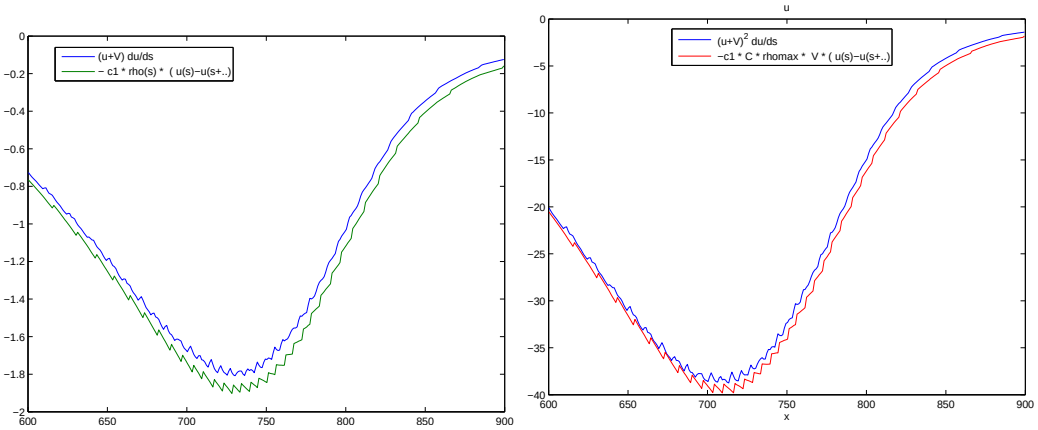


Figure 6: Left: Graph of the function $x \to (u(x,t)+V)\frac{\partial u}{\partial x}(x,t)$ and $x \to -c_1\rho(x,t)(u(x,t) - u(x+H - \tau V + Tu(x,t),t))$ at tme $t = 20sec$ as approximation of equation (10). Right: Graph of the function $x \to (u(x,t)+V)^2\frac{\partial u}{\partial x}(x,t)$ and $x \to -c_1 C\rho_{max}(u(x,t) - u(x+H-\tau V + Tu(x,t),t))$ at tme $t = 20sec$ as approximation of equation (11) and with $c_0 = C\rho_{max}$. In both cases the partial derivative is computed numerically using finite differences.

Finally, we used the numerical data set (for $\rho_0 = .26, V = 5.65$) to test the solutions provided by the localized jam equation (13). Figure 7 addresses the various ways of computing $\rho$.

We show the data for $\rho$ obtained from the full simulation, the $rho$ obtained by the match $\frac{c_0 V}{u+V}$ (where $u$ is taken from the simulation), and the match $\frac{c_0 V}{u+V}$ with $u$ taken as a solution of the localized jam equation (13). This solution is obtained by numerical integration using a standard fourth order Runge–Kutta method. As initial values we used $u(750) = 13, u'(750) = -0.08$ as obtained from the data set. The point $x = 750$ corresponds to the point of maximal absolute braking force in the full simulation. Figure 7 shows also the corresponding comparisons for $u$.

Three things are transparent: First, the original $\rho$ cannot correspond to a traveling wave for $x > 900$, as $\rho$ reaches a maximum and starts to decrease. This is a trivial consequence of the fact that our initial values for the full simulation are not compatible with a traveling wave solution on the whole domain. Second, the data match to $\rho$ is excellent for $x \in [600, 850]$, showing the traveling wave profile in this domain. Third, the traveling wave profile provided by the localized jam equation is a poor approximation to the true profile. This latter point is not surprising as we already observed that the Taylor approximation is rough because of the significant size of the nonlocalities.

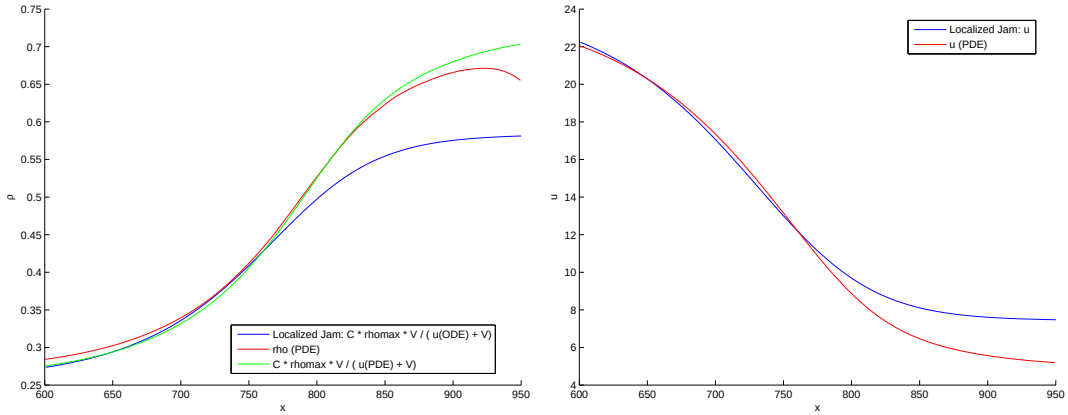


Figure 7: Comparison of different computations of $\rho$ (left) and $u$ (right). We present computations based on the full simulation of the partial differential equation (PDE) (23) and solutions to the localized jam equation (ODE) (13). The constant $C\rho_{max} = c_0$ is the best match of $u$ and $\rho$ to the jam equation (10). The solutions to (13) are computed with initial data prescribed at $x = 750m$. This is the point of maximal braking force in the solution to (23).

We repeated the same experiments for smaller $\rho$ and found larger errors (not surprising, as the traveling wave approximation is poorer). These pictures are omitted.

### 4.1.3 Comparison of Model Predictions

We next compared the effect of the modification of the braking term in (24) with simulations of the original model (23). We prescribe for the current simulations a constant velocity profile and we perturbe the density profile as depicted in Figure 8. The perturbation is chosen such that the modified braking term (24) is initially active only close to $x = 1000$. It remains active close to the peak of the density and is inactive elsewhere.

We chose $N_x = 4000$ grid points, $c_3 = 2.5$ and the remaining parameters as in Table 1. Only small changes in the qualitative shape of $\rho$ due to the model modifications were observed. But one easily sees that the shape of the emerging velocity profile is completely different. Whereas in the original model the velocity stays constant and the density is simply advected with this velocity, the modified

model exhibits braking scenarios and a decrease in the velocity around the state of high density. The perturbation has here acted as a trigger for a traveling wave solution.

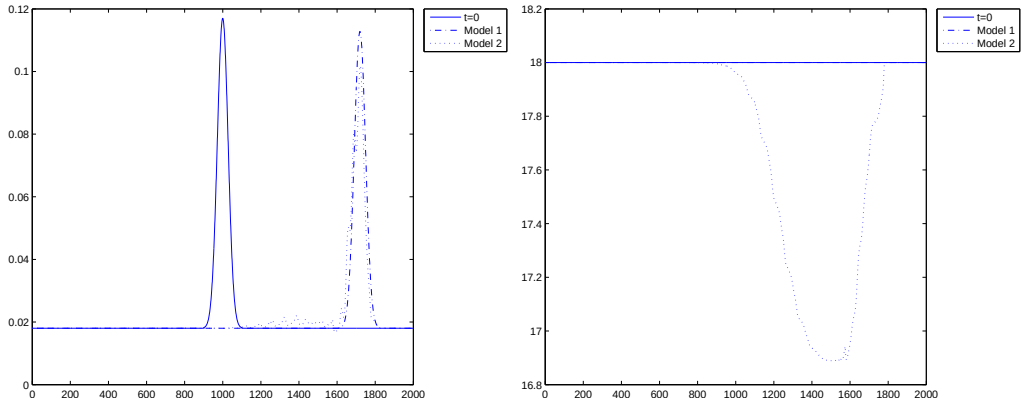


Figure 8: Density (in percentage of $\rho_{\max}$) and velocity profiles (in $m/s$) at $T = 40sec$ for different initial values of the densities. Model 1 refers to the original model (23) and model 2 to its modification (24).

#### 4.1.4 Explaining Density Oscillations (c.f. Remark 1)

Consider the following unrealistic scenario. Set (the safety distance) $H = 100$ and use constant initial density at 40% of $\rho_{\max}$ and a velocity of $21m/s$. Assume that for 5 seconds all cars in the interval $I = [900, 1100]$ brake according to equation (25) with $u^{lim} = 15m/s$. For $t \geq 5$ $sec$ the rule (24) is applied with $c_3 = 5$. We present snapshots of the solution for $t \in [0, 10]$ seconds in Figure 9. Clearly, in the first seconds all cars in the interval $I$ brake, and we observe a decrease in their speeds (green line). In the time interval after the first drivers react (i.e., after reaction time $\tau = 1$ $sec$) we observe that not only the cars in $I$ brake, but also cars in the range of $x \geq 800m$, since they observe the previously mentioned cars and adjust their velocity accordingly. As the braking force for those cars is proportional to $u - u^X$ and $u^X$ is the minimal speed of the lead cars, all cars in the range of $800 - 900$ brake with the same force. This yields the plateau shaped solution at time $t = 3$ $sec$ (red). Wherever $u$ exhibits "steps" we observe a peak in the density due to the continuity equation: $\rho_t = -\rho_x u - u_x \rho$. These pinches in the density advect and therefore remain throughout the simulation. The pattern repeats: The velocity profile at $t = 5$ $sec$ exhibits three areas of steps and three corresponding peaks in the density. This continues for later times $t$ and yields the oscillations in the density. For smaller $H$ the wavelength of the oscillations will be shorter.

### 4.2 Numerical Results on Triggers

We present numerical results for different triggers. In all simulation results we observe a backwards moving wave in the velocity and density profile. This travelling wave is considered as traffic jam. In the density we furthermore observe oscillations of high frequency with small amplitude. Their presence has been discussed in Remark 1 and Section 4.1.4.

#### 4.2.1 Perturbation of the Initial Density as Trigger of Traffic Jams

We consider a circular road and the braking term (24). The density is also assumed to be constant with a perturbation on a window of length $200m$ centered around $x = 1000m$. Contrary to the simulations

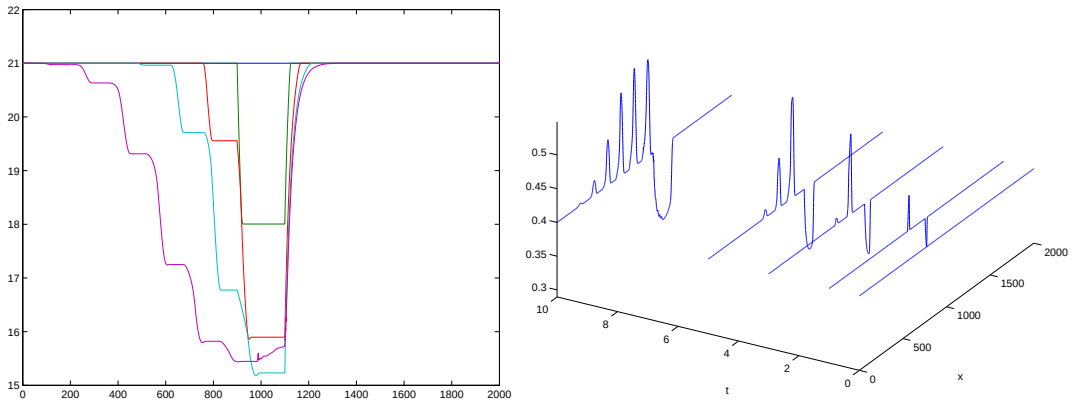


Figure 9: Density (in percentage of $\rho_{\max}$) and velocity profiles (in $m/s$) at $T = 40\ sec$

in Section 4.1.2 we prescribe an initially constant velocity of $u_0 = 18m/s$ for the full spatial interval. The situation modelled by this scenario is the occurrence of a sudden traffic accident leading to a higher density at some point of the road. At time $t = 0$ this accident is not yet recognzied by the drivers following.

The modified braking term (24) is equivalent to the original braking term (23) whenever $\rho^X(H + Tu) \leq c_3 = 2.5$. The regions wherein the modified braking term is active vary in time and space. For the simulation with an initial density of 20% of $\rho_{\max}$ the quantity $\rho^X(H + Tu)$ stays between 0.86 and 4.44 depending on spatial and temporal position.

The results are depicted in Figure 10. We observe the emergence and evolution of waves in the velocity profile depending on the initial density on the road and its perturbation. The initial density was varied from 5% of $\rho_{\max}$ to 22.5% of $\rho_{\max}$. The peak value of the perturbation was always 5.5 times the initial density, which guarantees that in the area of the higher density the modified braking force $-c_1\rho u$ acts. For a low initial density there is, over time, a decay in the density to a regime where the original braking law (23) applies. Depending on the initial level of $\rho$ we observe either forward moving waves (becoming steeper as time grows) in the velocity or backwards moving waves of travelling wave shape as in figure 10. The velocity decays at most by 3.5 $m/s$ corresponding to 12.6 $km/h$.

### 4.2.2 A Speed Limit as Trigger for Traffic Jams

We model a velocity constraint area by modifying the braking and acceleration scenario inside an interval $I$ where the constraint is active. Outside of $I$ we use (23), so that

$$B(x, \rho, u, u^X) = \begin{cases} -c_1\rho(u - u^{lim}) & x \in I. \\ -c_1\rho(u - u^X) & u - u^X > 0 \quad x \notin I \\ -c_2(\rho_{\max} - \rho)(u - \bar{u}^X) & u - u^X < 0 \quad x \notin I. \end{cases} \tag{25}$$

We start with initial constant densities in the range of $10\% - 40\%$ of the maximal density and constant velocity of $24m/s$. A velocity constraint $u^{lim} = 15m/s$ is imposed on a strip $I$ of length $200m$. As always, we study the arising wave patterns. A graph the solution is given in Figure 11.

### 4.2.3 Sudden Changes in the Velocity as Trigger for Traffic Jams

Here we use the braking and acceleration term (23) and consider a circular road with the parameters of table 1. For a duration of $5sec$ drivers in the interval $I = 990 - 1010m$ brake towards a limiting velocity

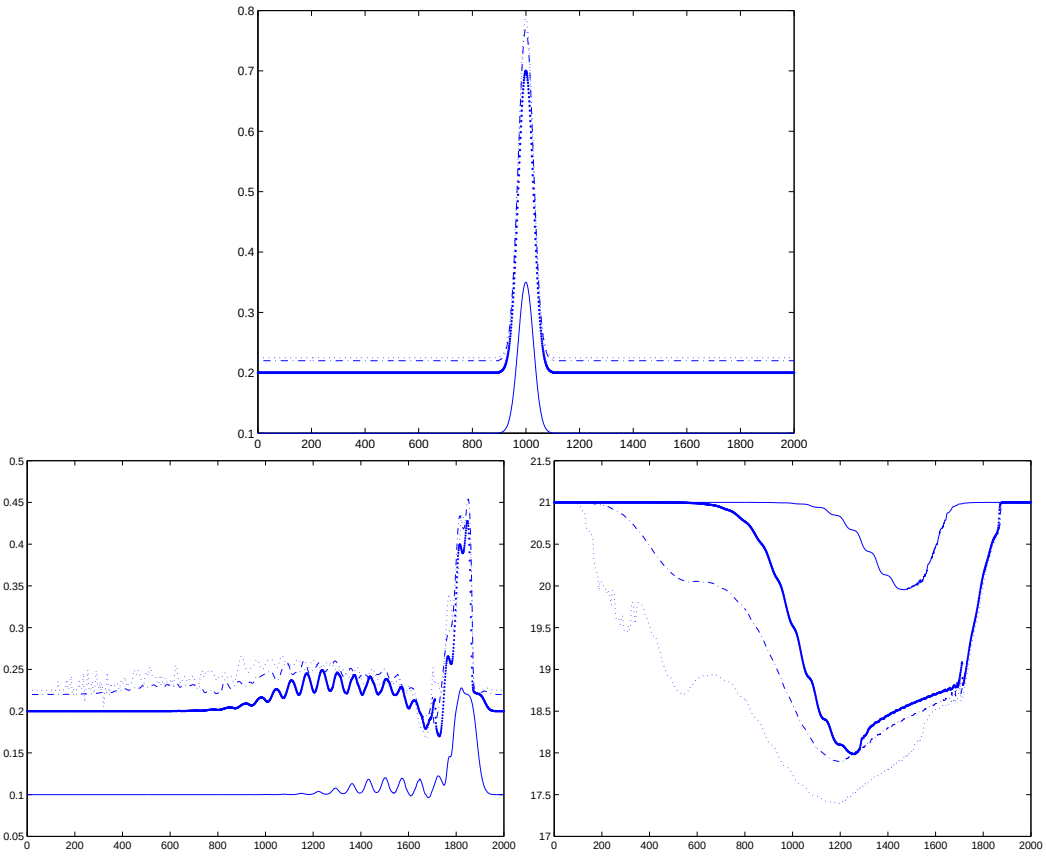

Figure 10: Bottom part of the picture: Density (in percentage of $\rho_{\max}$) and velocity profiles (in $m/s$) at $T = 40sec$ for different initial values of the densities. Initial data is depicted in the top part.

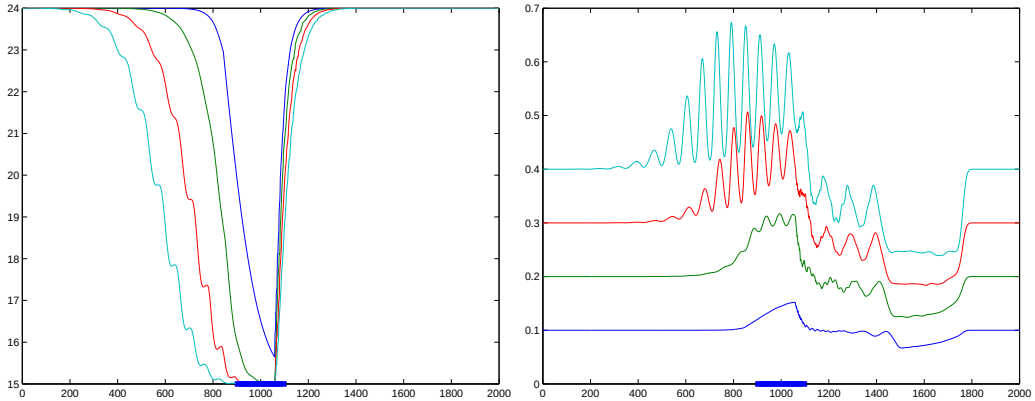

Figure 11: Density (in percentage of $\rho_{\max}$) and velocity profiles (in $m/s$) at $T = 30sec$ for different initial values of the densities. The bold part indicates the active velocity constraint which is set to $u_{lim} = 15m/s$. on a strip of $200m$ centered at $x = 1000m$.

of $u^{lim} = 15m/s$ according to (25). Then, for $t \geq 5\ sec$, the original rule (23) applies to all drivers. The solution is depcited in Figure 12.

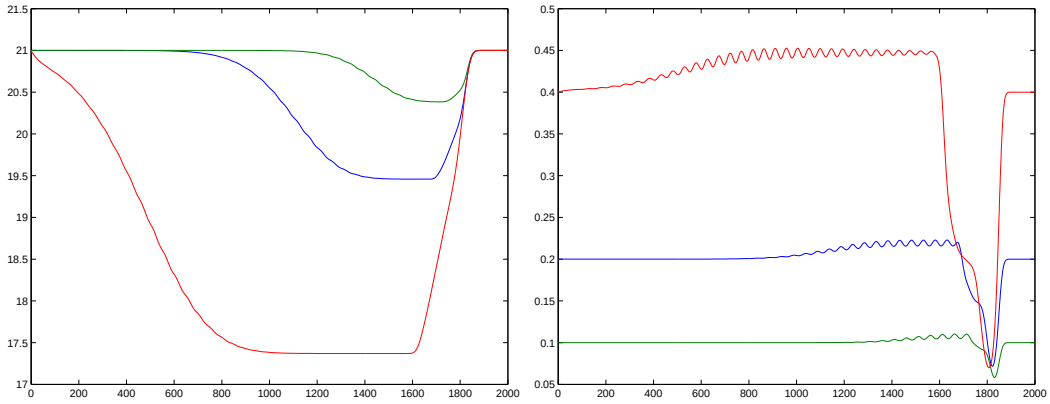


Figure 12: Density (in percentage of $\rho_{\max}$) and velocity profiles (in $m/s$) at $T = 40sec$

## Acknowledgments

This work has been supported by Seed Funds (RWTH Aachen), HE5386/6-1 and DAAD PPP D/08/11076, and by Discovery grant No. 7847 of the Natural Sciences and Enginerring Research Council of Canada.

## References

[1] A. Aw and M. Rascle, *Resurrection of "second order" models of traffic flow.*, SIAM J. Appl. Math., 60 (2000), pp. 916–938.

[2] A. Chertock, A. Kurganov, Y. Rykov, *A New Sticky Particle Method for Pressureless Gas Dynamics*, SIAM J. on Numerical Analysis, Vol. 45 (2007), pp. 2408–2441

[3] G. M. Coclite, M. Garavello and B. Piccoli, *Traffic flow on a road network*, SIAM J. Math. Anal., 36 (2005), pp. 1862–1886.

[4] C. F. Daganzo, *The cell transmission model : A dynamic representation of highway traffic consistent with the hydrodynamic theory*, Transp. Res. B, 28 (1994), pp. 269-287.

[5] J. Dolbeault and R. Illner, *Entropy methods for kinetic models of traffic flow*, Commun. Math. Sci, 1 (2003), pp. 401–423.

[6] I. Gasser, T. Seidel, G. Sirito, and B. Werner, *Bifurcation Analysis of a Class of Car Following Traffic Models II: Variable Reaction Times and Agressive Drivers*, Bulletin of the Institute of Mathematics, Academica Sinica (New Series), 2 (2007), pp. 587–607.

[7] I. Gasser, G. Sirito, and B. Werner, *Bifurcation analysis of a class of 'car following' traffic models.*, Physica D, 197 (2004), pp. 222–241.

[8] J. Greenberg, *Extensions and amplifications of a traffic model of Aw and Rascle.*, SIAM J. Appl. Math., 62 (2001), pp. 729–745.

[9] ——, *Congestion redux.*, SIAM J. Appl. Math., 64 (2004), pp. 1175–1185.

[10] ——, *Traffic congestion – an instability in a hyperbolic system*, Bulletin of the Institute of Mathematics, Academica Sinica (New Series), 2 (2007), pp. 123–138.

[11] J. Greenberg, A. Klar, and M. Rascle, *Congestion on multilane highways.*, SIAM J. Appl. Math., 63 (2003), pp. 818–833.

[12] R. Herman, I. Prigogine, *A two-fluid approach to twon traffic*, Science, Vol. 204 (1979), oo. 148-151

[13] D. Helbing, *Traffic dynamics. New physical concepts of modelling. (Verkehrsdynamik. Neue physikalische Modellierungskonzepte.)*, Berlin: Springer. xii, 308 p. DM 128.00; öS 934.40; sFr 113.00 , 1997.

[14] D. Helbing, A. Hennecke, V. Shvetsov, and M. Treiber, *Micro- and macro-simulation of freeway traffic.*, Math. Comput. Modelling, 35 (2002), pp. 517–547.

[15] M. Herty, R. Illner,*On stop-and-go waves in dense traffic.*, Kinetic and Related Models 1(3)(2008), pp. 437-452.

[16] M. Herty, R. Illner, A. Klar, and V. Panferov, *Qualitative properties of solutions to systems of Fokker-Planck equations for multilane traffic flow.*, Transp. Theory Stat. Phys., 35 (2006), pp. 31–54.

[17] M. Herty and A. Klar, *Modelling, simulation and optimization of traffic flow networks*, SIAM J. Sci. Comp., 25 (2003), pp. 1066-1087.

[18] M. Herty and M. Rascle, *Coupling conditions for a class of second-order models for traffic flow.* , SIAM J. Math. Anal., 38 (2006), pp. 595-616.

[19] R. Illner, C. Kirchner, and R. Pinnau, *A derivation of the aw–rascle traffic models from fokker-planck type kinetic models*, Quarterly Appl. Math., 67(1) (2009), pp. 39–45

[20] R. Illner, A. Klar, and T. Materne, *Vlasov-Fokker-Planck models for multilane traffic flow.*, Commun. Math. Sci., 1 (2003), pp. 1–12.

[21] A. Klar, R .Wegener, *A hierarchy of models for multilane vehicular traffic. I. Modeling.*, SIAM J. Appl. Math., Vol. 3 (1999), pp. 983–1001

[22] B. Kerner, *The Physics of traffic*, Springer, Berlin, 2004.

[23] J. P. Lebacque, *Les modèles macroscopiques de trafic*, Annales des Ponts 67, 3rd trim, (1993), pp 28-45.

[24] R. LeVeque, *The dynamics of pressureless dust clouds and delta waves*, Journal Hyperbolic Differential Equations, Vol. 1 (2004), pp. 315–327

[25] M. Lighthill and J. Whitham, *On kinematic waves*, Proc. Roy. Soc. London Ser. A, 229 (1955), pp. 281–345.

[26] E. Ben-Naim, P. L. Krapinsky, S. Redner, *Kinetics of clustering in traffic flows*, Physical Rev. E 50(2), (1994) pp. 822–829.

[27] P. I. Richards, *Shock waves on the highway*, Oper. Res., 4 (1956), pp. 42–51.

[28] L. Santen, A. Schadschneider, M. Schreckenberg, *Towards a realistic microscopic description of highway traffic*, J. Phys A, Vol. 33, (2000), pp. 477–485

[29] S. Marinosson, R. Chrobok, A. Pottmeier, J. Wahle, M. Schreckenberg, *Simulation framework for the autobahn traffic in North Rhine-Westphalia*, Cellular automata 315–324, Lecture Notes in Comput. Sci., 2493, Springer, Berlin (2002)

[30] T. Alperovich, A. Sopasakis, *Stochastic description of traffic flow*, J. Stat. Phys., Vol. 133 (2008), pp. 1083-1105

[31] A. Sopasakis, M.A. Katsoulakis, *Stochastic modeling and simulation of traffic flow: asymmetric single exclusion process with Arrhenius look-ahead dynamics*, SIAM J. Appl. Math., Vol. 66 (2006), pp. 921-944.

[32] M. Treiber and D. Helbing, *Macroscopic simulation of widely scattered synchronized traffic states.*, J. Phys. A, Math. Gen., (1999).

[33] H. M. Zhang, *A non–equilibrium traffic model devoid of gas–like behavior*, Tans. Res. B, Vol. 36 (2002), pp. 275–290